Hybrid Device of Hexagonal Boron Nitride Nanoflakes with Defect Centres and a Nano-Fibre Bragg Cavity

Toshiyuki Tashima
Kyoto University
Hideaki Takashima
Kyoto University
Andreas W. Schell
Leibniz University Hannover
Toan Trong Tran
University of Technology Sydney
Igor Aharonovich
University of Technology Sydney
Shigeki Takeuchi (takeuchi@kuee.kyoto-u.ac.jp)
Kyoto University

Research Article

Keywords: nanofibre Bragg cavities (NFBCs), focused ion beam (FIB),

Posted Date: August 4th, 2021

DOI: https://doi.org/10.21203/rs.3.rs-761412/v1

Version of Record: A version of this preprint was published at Scientific Reports on January 7th, 2022.
See the published version at https://doi.org/10.1038/s41598-021-03703-z.

Hybrid device of hexagonal boron nitride nanoflakes with defect centres and a nano-fibre Bragg cavity

Toshiyuki Tashima[1], Hideaki Takashima[1], Andreas W. Schell[2,3], Toan Trong Tran[4], Igor Aharonovich[4,5], and Shigeki Takeuchi[1,*]

[1]Department of Electronic Science and Engineering, Kyoto University, 615-8510 Kyoto, Japan
[2]Faculty of Mathematics and Physics, Leibniz University Hannover, 30167 Hannover, Germany
[3]Physikalisch-Technische Bundesanstalt, 38116 Braunschweig, Germany
[4]School of Mathematical and Physical Sciences, University of Technology Sydney, Ultimo, New South Wales 2007, Australia
[5]ARC Centre of Excellence for Transformative Meta-Optical Systems (TMOS), University of Technology Sydney, Ultimo, New South Wales 2007, Australia
[*]takeuchi@kuee.kyoto-u.ac.jp

ABSTRACT

Solid-state quantum emitters coupled with a single mode fibre are of interest for photonic and quantum applications. In this context, nanofibre Bragg cavities (NFBCs), which are microcavities fabricated in an optical nanofibre, are promising devices because they can efficiently couple photons emitted from the quantum emitters to the single mode fibre. Recently, we have realized a hybrid device of an NFBC and a single colloidal CdSe/ZnS quantum dot. However, colloidal quantum dots exhibit inherent photo-bleaching. Thus, it is desired to couple an NFBC with defect centres in hexagonal boron nitride (hBN) as stable quantum emitters. In this work, we realize a hybrid system of an NFBC and defect centres in hBN nanoflakes. In this experiment, we fabricate NFBCs with a quality factor of 807 and a resonant wavelength at around 573 nm, which matches well with the fluorescent wavelength of the defect centres in hBN, using a helium focused ion beam (FIB) system. We also develop a manipulation system to place hBN nanoflakes on a cavity region of the NFBCs and realize a hybrid device with an NFBC. By exciting the nanoflakes via an objective lens and collecting the fluorescence through the NFBC, we observe a sharp emission peak at the resonant wavelength of the NFBC.

Introduction

Photonic quantum technologies, such as photonic quantum computing and quantum sensing, have attracted considerable attention recently. In realizing these technologies, it is important to couple photons to single-mode optical fibres without connection loss. In this context, solid-state quantum emitters coupled with single mode fibres are of interest. Especially, optical nanofibres[1,2], which are tapered fibres with a diameter less than the wavelength of the propagation light at the tapered waist, are promising. A nanofibre has a high transmittance of almost unity, lossless interconnection to single mode fibres, and a large evanescent field in the tapered waist, and can efficiently couple photons emitted from quantum emitters on the surface to a single mode fibre with a coupling efficiency of about 30%[3,4]. Coupling of various kinds of solid-state quantum emitters with optical nanofibres has been demonstrated[3,5–9].

Although the coupling efficiency of 30% is high, further improvement of the coupling efficiency toward 100% is desirable. For this purpose, nanofibre Bragg cavities (NFBCs), which are optical microcavities embedded in a nanofibre, have recently been proposed and demonstrated[10–14]. NFBCs have a single resonant mode with a small mode volume (on the order of the cube of the wavelength), high quality (Q) factors, ultra-wide tunability of the resonant wavelength, and lossless coupling to single-mode fibres[11]. Furthermore, we demonstrated the enhancement of photon emission from a single colloidal CdSe/ZnS quantum dot coupled with an NFBC[11]. However, the inherent photo-bleaching and blue-shift of the emission wavelength of colloidal quantum dots are problems. Moreover, the linewidth of the emission peak is typically more than 10 nm at room temperature, which is too broad for the resonant linewidth of an NFBC with a reasonable Q factor. Therefore, it is desired to couple stable and robust quantum emitters with a narrow emission peak to NFBCs.

For these quantum emitters, a thin layered material composed of hexagonal boron nitride (hBN) with defect centres has attracted attention. These emitters exhibit ultra-bright single photon emission with a quantum efficiency of over 90 %[15] and high robustness[16]. The defect centres in hBN show sharp emission peaks with line widths less than 5 nm at room temperature[17–20] and a few nm at cryogenic temperature[21–24]. In addition to basic optical characteristics investigations, two-photon absorption

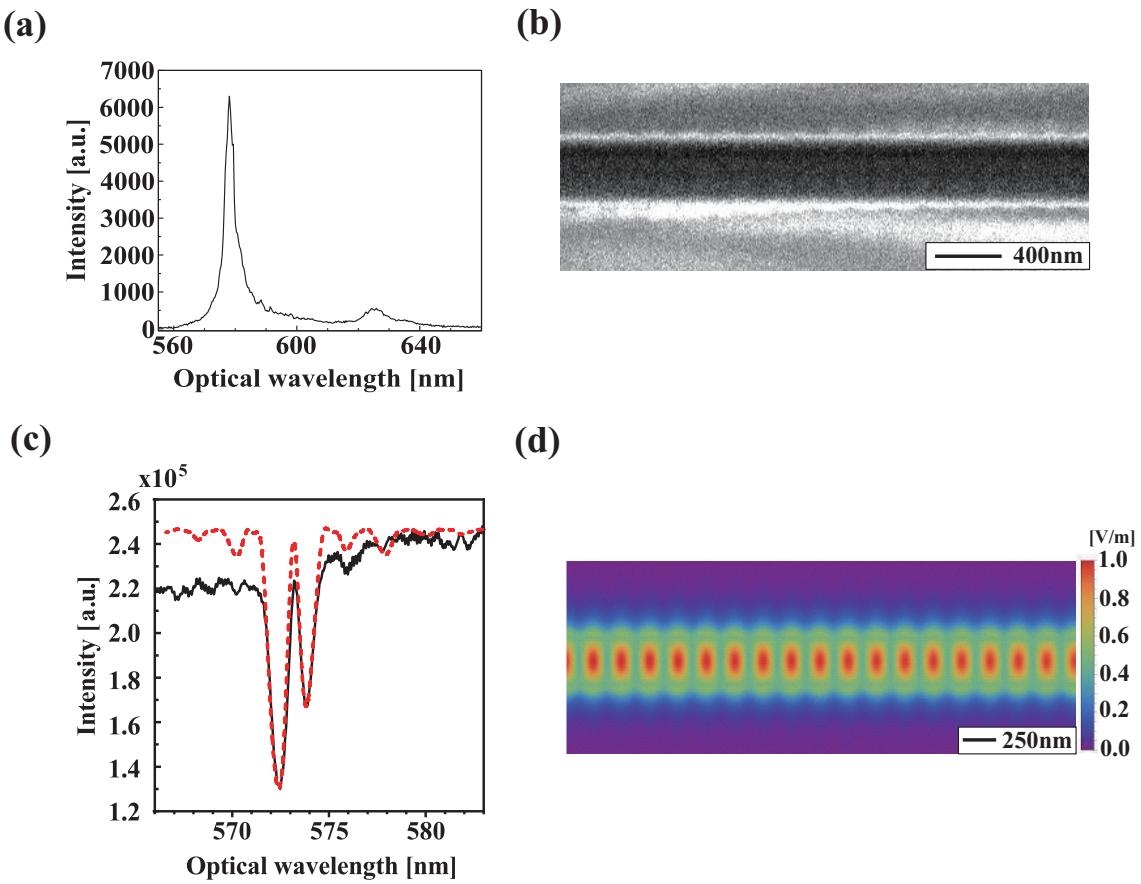

Figure 1. (a) Example emission spectrum from defects in hBN. (b) SIM image of the fabricated NFBC. The fabricated NFBC appears black due to the charge-up. (c) Spectra of the fabricated NFBC (black line) and numerical curve (red dotted line). The resonant wavelength is 573 nm, and the linewidth is 0.71 nm. (d) Distribution of electric field intensity at the resonant wavelength of the NFBC. The two-way arrow indicates the dipole direction.

using near-infrared lasers[25] and anti-Stokes excitation[26] has been realized. Also, a three-dimensional analysis of the dipole orientation of a single defect centre in hBN has been experimentally performed.[15,27]. Moreover, the defect centres in hBN have been coupled to nanophotonic devices, such as optical nanofibres, waveguides, metamaterials, and photonic crystals[28–32].

In this paper, we report on the experimental realization of a hybrid device of NFBCs and defect centres in hBN nanoflakes. In this experiment, we fabricate NFBCs with a Q factor of 807 and a resonant wavelength at around 573 nm, which almost matches the fluorescent wavelength of the defect centres, by a helium focused ion beam (FIB) system. Using the helium FIB, the problem of residual ions in the device, exhibited by a previous device created using a gallium FIB, has been solved, resulting in better resonator characteristics[33]. A hybrid device with an NFBC and defect centres in hBN nanoflakes is then realized by picking and placing the hBN nanoflakes on a cavity region of the NFBC using a custom-made manipulation system. Finally, we confirm a sharp emission peak at the resonant wavelength of the NFBC when we excite the nanoflakes in the hybrid device via an objective lens and detect the photons through the fibre output of the device.

Results and discussion

Optical properties of defects in hBN nanoflakes

We evaluate the optical properties of defect centres in the hBN nanoflakes used in our experiment. The defect centres are introduced into the nanoflake by annealing at 850 ° C for 30 min under 1 Torr of argon atmosphere[28]. The observed spectrum of our samples typically shows two peaks: one is the ZPL at around 575 nm ±10 nm and the other is a phonon sideband at around 625 nm ±10 nm, as shown in Fig. 2(a). The size of the sample is roughly 1 μm–2 μm. We also find that the second-order autocorrelation function, $g^{(2)}(0)$, is almost unity. Thus, it is considered that the defect centres in our samples on the substrate are a typical ensemble.

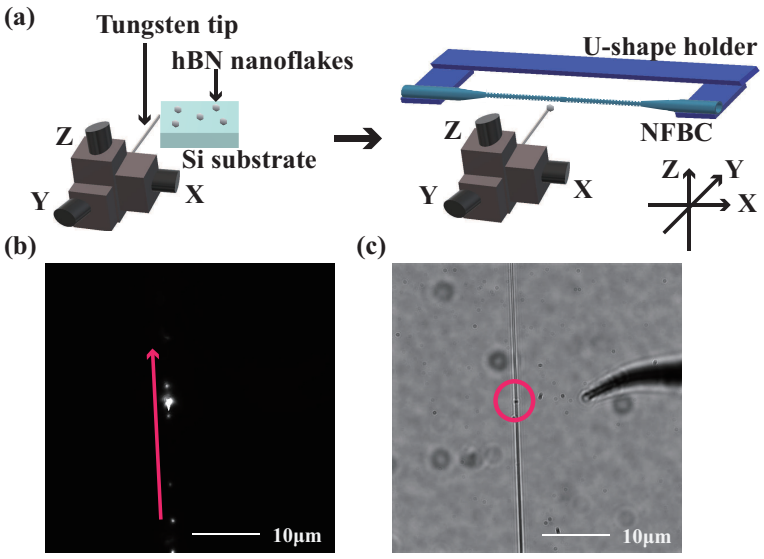

Figure 2. (a) Pick and place system for hBN nanoflakes. The left side illustrates the process for picking up an hBN nanoflake on a Si substrate by a tungsten tip on an XYZ stage. The right side illustrates placing the hBN nanoflake on an NFBC by the tungsten tip. The NFBC is fixed by a U-shape holder. (b) CCD image of the NFBC with a white light source. The bright spot is the centre of the NFBC. The red arrow indicates the direction of the nanofibre. (c) CCD image after placing the hBN nanoflake on the NFBC. The red circle indicates the hBN nanoflake on the NFBC. The tungsten tip can be observed on the right side of the nanofibre. (Black dots in the image show dirt on the surface of the CCD camera.)

Optical properties and numerical analysis of the fabricated NFBCs

Based on the above results, we select the ZPL with a centre wavelength of 575 nm as the resonant wavelength of the NFBC. We fabricate an optical nanofibre with a waist diameter of $\sim$ 400 nm by heating a single-mode optical fibre (Thorlabs 630HP) with a ceramic heater and stretching it into a fine thread while maintaining single-mode propagation. The nanofibre is fixed on a U-shape metal holder, shown in Fig. 2(a). Using a He-ion FIB system with a fabrication resolution of less than 1 nm (Zeiss, Orion NanoFab)[33], we fabricated a cavity structure on the nanofibre with a resonant wavelength close to the centre wavelength of 575 nm . A scanning ion microscope (SIM) image of the fabricated NFBC is shown in Fig. 1(b). We observe faint periodic grooves at $\sim$ 200 nm spacing on the fabricated nanofibre. The transmission spectrum (black color) of this fabricated NFBC is shown in Fig. 1(c). The resonant wavelength is 573 nm, and the line width of this peak is 0.71 nm, with a Q-value of $\sim$ 807. The reduction of the transmission at the shorter wavelength side is due to the intensity dependence of the white light used as a light source. To evaluate the fabricated NFBC, we numerically simulate the transmission spectra and electric field intensity based on a three-dimensional (3D) finite-difference time-domain (FDTD) simulation (see methods). The numerically simulated spectrum (red dotted color) almost corresponds to the experimental spectrum as shown in Fig. 1(c). The distribution of electric field intensity at this resonant wavelength is shown in Fig. 1(d). The electric field intensity approaching the centre of the cavity increased with a period of 236.4 nm. In this way, we succeeded in fabricating an NFBC with a resonant wavelength close to the centre wavelength of the ZPL of the defect centres in hBN.

Transferring the hBN nanoflakes onto the NFBCs

We transfer a nanoflake to the fabricated NFBC using a sharp tungsten tip manipulated by a three-axis stage, as shown in Fig. 2(a). First, the tungsten tip set on the stage is directed to the silicon substrate with the dispersed nanoflake. The nanoflake is picked up onto the tip and then placed at the centre point of the NFBC (bright spot in Fig. 2(b)) under observation using a CCD camera while propagating the light of the white light source in the NFBC. Figure 2(c) shows a CCD camera image of the NFBC after transferring an hBN nanoflake onto it. The nanoflake is observed as a small round dot in the red circle. This position of the dot is the same as the bright spot in Fig. 2(b). From this picture, the size of nanoflakes is estimated to be about 1.5 μm. Note that the tungsten tip is also observed in the CCD camera image of Fig. 2(c).

Hybrid device of defect centres in hBN nanoflakes coupled to an NFBC

We characterize the photoluminescence from defect centres in a nanoflake on an NFBC using a confocal microscope system (see Methods). The experimental setup is shown in Fig. 3(a). Figure 4(a) shows a confocal microscope image when the nanoflake is excited through the objective lens and the emitted photons are collected with the same objective lens. A bright spot

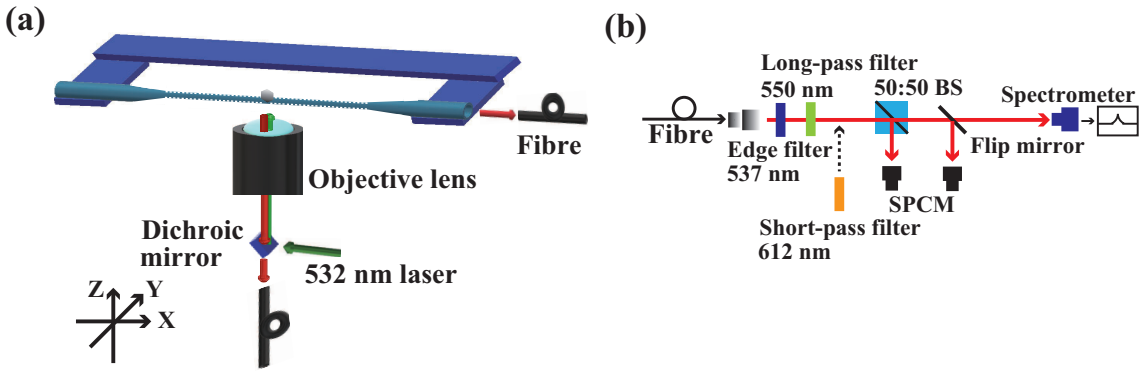

Figure 3. (a) Confocal microscope system for estimating an hBN nanoflake. A dichroic mirror separates the excitation light and the light emitted from the defect centres in hBN. (b) Detection system. A 537 nm edge filter and a 550 nm long-pass filter are placed before a 50:50 beam splitter (50:50 BS), single-photon counting modules (SPCMs), and a spectrometer. A 612 nm short-pass filter is inserted when the emission light is observed via the fibre end of the NFBC.

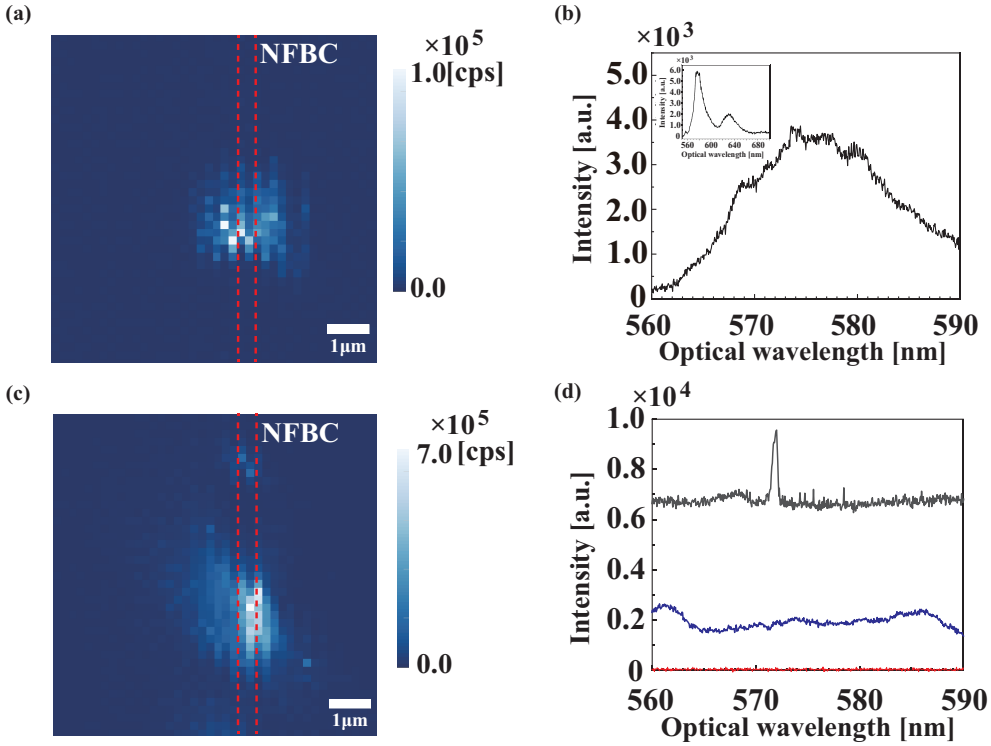

Figure 4. (a) Scanning image and (b) spectrum of the emission light from defect centres in an hBN on an NFBC via an objective lens. The region is around the centre wavelength of 575 nm on ZPL. The inset is the spectrum of all emission light from the defect centres. (c) Scanning image and (d) spectrum of the emission light from the defect centres in hBN via the fibre end (black curve). A sharp peak is observed around 572.6 nm. The blue curve shows the spectrum of background light without the nanoflake via the fibre end. The red line shows the spectrum of the emission light from only the NFBC via the fibre end, without the hBN nanoflake. These are excited by a pump laser through an objective lens. The red dotted line in Figs (a) and (c) is the position of the NFBC.

with a full width at half-maximum (FWHM) of about 1.3 μm is observed on the estimated position of the nanofibre (red dotted line). The spread of this bright spot is likely to be due to the size of the nanoflake $\sim$ 1.5 μm, which is estimated from the CCD camera image in Fig. 2(c), and small vibrations of the nanofibre. We measure all emission spectrum of this bright spot, shown in the inset of Fig. 4(b). Two emission peaks at λ = 575 nm and 630 nm are observed in the spectrum. The positions of the peaks almost agree with the typical wavelengths of the emission peaks from the nanoflake on the silicon substrate, as shown in Fig. 1(a). However, the linewidth of the peak is broader than the example in Fig. 1(a), likely due to the number of hBN layers[18] and the size and shape of each nanoflake. To estimate the number of defect centres, we measure the second-order correlation function $g^2(\tau)$. $g^{(2)}(0)$ is almost unity, which means that the number of defect centres is much higher than one. In this way, we can confirm that an hBN nanoflake with defect centres is transferred to the NFBC from the Si substrate.

To confirm the coupling of the defect centres in the hBN nanoflake to the NFBC, we characterize the fluorescence through one end of the NFBC. Figure 4(c) shows a scanning image. A bright spot is observed at almost the same position as the nanoflake when the fluorescence is collected using the objective lens, shown in Fig. 4(a). The shape of the bright spot looks like an ellipse along the NFBC (x-axis in Fig. 3(a)). The FWHMs in the vertical and horizontal directions are 1.8 μm and 0.9 μm, respectively. Since the photons from the emitters are coupled to the nanofibre via the evanescent field ($\sim \lambda$) on the NFBC, it is considered that the length of the horizontal FWHM should be shorter than the vertical length. A black line in Fig. 4(d) shows an emission spectrum when the bright spot is excited, and the fluorescence is measured via the NFBC. Compared with the spectrum in Fig. 4(b), a sharp emission peak at a wavelength of 572.6 nm is observed over the background light with almost constant intensity. This peak wavelength almost agrees with the resonant wavelength of the NFBC of 573 nm (Fig. 1(c). The difference of 0.4 nm may be due to the temperature shift of 0.67 nm/°C during the experiment. In this way, we have realized a hybrid device of defect centres in hBN nanoflakes and an NFBC.

Finally, to clarify the source of the large background light with almost constant intensity in the emission spectrum of the black curve in Fig. 4(d), we investigate an NFBC without a hBN nanoflake and an NFBC with a defect-free hBN nanoflake. The red line in Fig. 4(d) shows the emission spectrum when the NFBC without an hBN nanoflake is excited with an excitation power of 150 μW and the fluorescence is collected via the NFBC. The intensity of the spectrum is almost zero in the range of the observed wavelength. That is, we observe no fluorescence when only the NFBC was excited. Next, we investigate the NFBC with a defect-free hBN nanoflake. Note that this NFBC has a resonant wavelength of 577 nm and FWHM of 0.7 nm. The blue curve in Fig. 4(d) shows the emission spectrum when the fluorescence is measured via one end of the NFBC. A spectrum with almost constant intensity is observed. We consider that this is due to the fluorescence of the impurities existing in the single-mode fibre, excited by the pump light coupled to the nanofibre via nanoflakes as a scatterer. The difference in the intensity between the blue curve and the background level of the black curve is considered due to the difference in the coupling efficiency of the pump light to the nanofibre caused by the shape and size of the nanoflake. To suppress this large background emission, it may be useful to use smaller hBN nanoflakes.

Conclusion

In conclusion, we have experimentally demonstrated a hybrid device of an NFBC and an hBN nanoflake with defect centres. We also observed a sharp emission peak at the resonant wavelength of 573 nm for the NFBC, close to the centre wavelength of 575nm for the ZPL of defect centres in an hBN nanoflake. Our results open up a new direction of coupling photons emitted from stable quantum emitters with the narrow ZPL wavelength in defect centres into a single mode fibre, toward the realization of a fibre-integrated quantum information platform.

Methods

Numerical simulation for the fabricated NFBC

We numerically simulate the transmission spectra and electric field intensity based on a three-dimensional (3D) finite-difference time-domain (FDTD) simulation[12] using a commercial package (FDTD Solutions, Lumerical). The calculation area for the FDTD simulation is set to 120 $\times$ 2 $\times$ 2 μm^3. The diameter of the nanofibre and the depth of the groove used in the calculation model are set to 400 nm and 10 nm, respectively. These parameters are estimated from the SIM image in Fig. 1(b). The period of the grating and the length of the defect are set to 236.4 nm and 700.7 nm, respectively. The refractive indexes of the nanofibre and the parts of the nanofibre implanted with He ions[34] are set to 1.45855 and 1.4555, respectively.

Experimental setup

The experimental setup is shown in Fig. 3(a). We use a 532 nm laser with an excitation power of 250 μW. The light from the laser is reflected by a dichroic mirror onto the nanoflake via an objective lens for optical excitation. The fluorescence from the defect centres in the nanoflake is collected through the objective lens and the NFBC. After passing through the dichroic mirror, the fluorescence is collected with another objective lens, simplified in the diagram, and coupled to a multi-mode fibre with a

core diameter of about 10 μm toward the detection system in Fig. 3(b). Also, the fluorescence passing through the NFBC goes directly to the detection system. The detection system consists of a 537 nm edge filter and a 550 nm long-pass filter to cut the excitation light. We also use a 50:50 beam splitter (50:50 BS), single photon counting modules (SPCMs) to observe the scanning image and the second-order autocorrelation function, $g^{(2)}(\tau)$, and a spectrometer.

References

1. Nayak, K. P. *et al.* Optical nanofiber as an efficient tool for manipulating and probing atomic fluorescence. *Opt. Express* **15**, 5431–5438, DOI: 10.1364/OE.15.005431 (2007).
2. Takeuchi, S. Taper optical fiber (2010).
3. Liebermeister, L. *et al.* Tapered fiber coupling of single photons emitted by a deterministically positioned single nitrogen vacancy center. *Appl. Phys. Lett.* **104**, 031101, DOI: 10.1063/1.4862207 (2014).
4. Almokhtar, M., Fujiwara, M., Takashima, H. & Takeuchi, S. Numerical simulations of nanodiamond nitrogen-vacancy centers coupled with tapered optical fibers as hybrid quantum nanophotonic devices. *Opt. Express* **22**, 20045–20059, DOI: 10.1364/OE.22.020045 (2014).
5. Fujiwara, M., Toubaru, K., Noda, T., Zhao, H.-Q. & Takeuchi, S. Highly efficient coupling of photons from nanoemitters into single-mode optical fibers. *Nano Lett.* **11**, 4362–4365, DOI: 10.1021/nl2024867 (2011). PMID: 21894938, https://doi.org/10.1021/nl2024867.
6. Yalla, R., Le Kien, F., Morinaga, M. & Hakuta, K. Efficient channeling of fluorescence photons from single quantum dots into guided modes of optical nanofiber. *Phys. Rev. Lett.* **109**, 063602, DOI: 10.1103/PhysRevLett.109.063602 (2012).
7. Schröder, T. *et al.* A nanodiamond-tapered fiber system with high single-mode coupling efficiency. *Opt. Express* **20**, 10490–10497, DOI: 10.1364/OE.20.010490 (2012).
8. Yonezu, Y., Wakui, K., Furusawa, K., Takeoka, M. & K. Semba and, T. A. Efficient single-photon coupling from a nitrogen-vacancy center embedded in a diamond nanowire utilizing an optical nanofiber. *Sci. Rep.* **7**, 12985, DOI: 10.1038/s41598-017-13309-z (2017).
9. Li, W., Du, J. & Chormaic, S. N. Tailoring a nanofiber for enhanced photon emission and coupling efficiency from single quantum emitters. *Opt. Lett.* **43**, 1674–1677, DOI: 10.1364/OL.43.001674 (2018).
10. Le Kien, F. & Hakuta, K. Cavity-enhanced channeling of emission from an atom into a nanofiber. *Phys. Rev. A* **80**, 053826, DOI: 10.1103/PhysRevA.80.053826 (2009).
11. Schell, A. W. *et al.* Highly efficient coupling of nanolight emitters to a ultra-wide tunable nanofibre cavity. *Sci Rep* **5**, 9619, DOI: 10.1038/srep09619 (2015).
12. Takashima, H., Fujiwara, M., Schell, A. W. & Takeuchi, S. Detailed numerical analysis of photon emission from a single light emitter coupled with a nanofiber bragg cavity. *Opt. Express* **24**, 15050–15058, DOI: 10.1364/OE.24.015050 (2016).
13. Tashima, T., Takashima, H. & Takeuchi, S. Direct optical excitation of an nv center via a nanofiber bragg-cavity: a theoretical simulation. *Opt. Express* **27**, 27009–27016, DOI: 10.1364/OE.27.027009 (2019).
14. Romagnoli, P., Maeda, M., Ward, J. M., Truong, V. G. & Chormaic, S. N. Fabrication of optical nanofibre-based cavities using focussed ion-beam milling: a review. *Appl. Phys. B* **126**, 111, DOI: https://doi.org/10.1007/s00340-020-07456-x (2020).
15. Nikolay, N. *et al.* Direct measurement of quantum efficiency of single-photon emitters in hexagonal boron nitride. *Optica* **6**, 1084–1088, DOI: 10.1364/OPTICA.6.001084 (2019).
16. Kianinia, M. *et al.* Robust solid-state quantum system operating at 800k. *ACS Photonics* **4**, 768–773, DOI: 10.1021/acsphotonics.7b00086 (2017).
17. I, A., Englund, D. & Toth, M. Solid-state single-photon emitters. *Nat. Photon* **10**, 631–641, DOI: 10.1038/nphoton.2016.186 (2016).
18. Tran, T. T., Bray, K., Ford, M. J., Toth, M. & Aharonovich, I. Quantum emission from hexagonal boron nitride monolayers. *Nat. Nanotech* **11**, 37–41, DOI: 10.1038/nnano.2015.242 (2016).
19. Grosso, G. *et al.* Tunable and high-purity room temperature single-photon emission from atomic defects in hexagonal boron nitride. *Nat Commun* **8**, 705, DOI: 10.1038/s41467-017-00810-2 (2017).
20. Vogl, T., Campbell, G., Buchler, B. C., Lu, Y. & Lam, P. K. Fabrication and deterministic transfer of high-quality quantum emitters in hexagonal boron nitride. *ACS Photonics* **5**, 2305–2312, DOI: 10.1021/acsphotonics.8b00127 (2018).

21. Jungwirth, N. R. *et al.* Temperature dependence of wavelength selectable zero-phonon emission from single defects in hexagonal boron nitride. *Nano Lett.* **16**, 6052–6057, DOI: 10.1021/acs.nanolett.6b01987 (2016). https://doi.org/10.1021/acs.nanolett.6b01987.

22. Sontheimer, B. *et al.* Photodynamics of quantum emitters in hexagonal boron nitride revealed by low-temperature spectroscopy. *Phys. Rev. B* **96**, 121202, DOI: 10.1103/PhysRevB.96.121202 (2017).

23. Dietrich, A. *et al.* Observation of fourier transform limited lines in hexagonal boron nitride. *Phys. Rev. B* **98**, 081414, DOI: 10.1103/PhysRevB.98.081414 (2018).

24. Duong, N. M. H. *et al.* Facile production of hexagonal boron nitride nanoparticles by cryogenic exfoliation. *Nano Lett.* **19**, 5417–5422, DOI: 10.1021/acs.nanolett.9b01913 (2019). PMID: 31264881.

25. Schell, A. W., Tran, T. T., Takashima, H., Takeuchi, S. & Aharonovich, I. Non-linear excitation of quantum emitters in hexagonal boron nitride multiplayers. *APL Photonics* **1**, 091302, DOI: 10.1063/1.4961684 (2016).

26. Tran, T. T., Bradac, C., Solntsev, A. S., Toth, M. & Aharonovich, I. Suppression of spectral diffusion by anti-Stokes excitation of quantum emitters in hexagonal boron nitride. *Appl. Phys. Lett.* **115**, 071102, DOI: 10.1063/1.5099631 (2019).

27. Takashima, H. *et al.* Determination of the dipole orientation of single defects in hexagonal boron nitride. *ACS Photonics* **7**, 2056–2063, DOI: 10.1021/acsphotonics.0c00405 (2020).

28. Schell, A. W., Takashima, H., Tran, T. T., Aharonovich, I. & Takeuchi, S. Coupling quantum emitters in 2d materials with tapered fibers. *ACS Photonics* **4**, 761–767, DOI: 10.1021/acsphotonics.7b00025 (2017).

29. Kim, S. *et al.* Photonic crystal cavities from hexagonal boron nitride. *Nat. Commun.* **9**, 2623, DOI: https://doi.org/10.1038/s41467-018-05117-4 (2018).

30. Glushkov, E. *et al.* Waveguide-based platform for large-fov imaging of optically active defects in 2d materials. *ACS Photonics* **6**, 3100–3107, DOI: 10.1021/acsphotonics.9b01103 (2019).

31. Baumberg, J. J., Aizpurua, J., Mikkelsen, M. H. & Smith, D. R. Extreme nanophotonics from ultrathin metallic gaps. *Nat. Mater.* **18**, 668–678, DOI: https://doi.org/10.1038/s41563-019-0290-y (2018).

32. Kim, S. *et al.* Integrated on chip platform with quantum emitters in layered materials. *Adv. Opt. Mater.* **7**, 1901132, DOI: 10.1002/adom.201901132 (2019). https://onlinelibrary.wiley.com/doi/pdf/10.1002/adom.201901132.

33. Takashima, H. *et al.* Fabrication of a nanofiber bragg cavity with high quality factor using a focused helium ion beam. *Opt. Express* **27**, 6792–6800, DOI: 10.1364/OE.27.006792 (2019).

34. Webb, A. P. & Townsend, P. D. Refractive index profiles induced by ion implantation into silica. *J. Phys. D: Appl. Phys.* **9**, 1343–1354, DOI: 10.1088/0022-3727/9/9/011 (1976).

Acknowledgements

This work was supported in part by a Grant-in-Aid for Scientific Research (21H04444, 26220712, 19K03700, 19K03686), the MEXT Quantum Leap Flagship Program (MEXT Q-LEAP) (JPMXS0118067634), the CREST program of the Japan Science and Technology Agency (JST) (JPMJCR1674), and the Nanotechnology Platform of MEXT (JPMXP09F20OS0018). The authors wish to thank the Australian Research Council (CE200100010) for financial support. A. W. S. was supported by Deutsche Forschungsgemeinschaft (DFG, German Research Foundation) under Germany's Excellence Strategy - EXC-2123 Quantum Frontiers - 390837967.

Author contributions statement

The experiment and the numerical calculation were carried out by T. T. and H. T.. T. T. T. and I. A. prepared the hBN nanoflakes. T. T., H. T., and S. T. wrote the paper and all authors discussed the experiment and text. S. T. supervised the study.